Remote sensing illustrates patterns of change and permanence in eelgrass meadows, False Bay Washington

Robert Hoekendorf
Biodiversity & Monitoring of Estuarine Ecosystems
Autumn 2021

Keywords: Seagrass, eelgrass, remote sensing, GIS, aquatic vegetation

Abstract

Seagrasses are an important global resource which serve as ecosystem engineers, providing a wide range of ecosystem functions and services. Unfortunately, many seagrasses such as eelgrass (*Zostera marina*) are declining in abundance worldwide due to multiple local and global stressors. Declines in eelgrass abundance cause concern for the habitats it exists in, due to the important biological roles seagrasses fill. Increasing ocean temperatures predicted to intensify under current climate change models may be contributing to this global decline of seagrasses. In order to investigate this relationship, historic changes in eelgrass extent were examined within False Bay located between San Juan Island and Haro Strait in the Salish Sea. Using remote sensing techniques and spatial analysis, changes in eelgrass extent were able to be quantified in ten different years spanning 1990 - 2021. The total area of observed eelgrass extent ranged from $8316m^2$ to $16120m^2$ with the greatest change occurring from 2015 to 2017 ($-7069m^2$). We investigated potential relationships between variability of eelgrass within the shallow subtidal zone, recorded air temperature and the Pacific decadal oscillation index (PDO). No consistent trend of increase or decrease in eelgrass extent was found over the entire study period. However, we found a positive correlation between eelgrass growth and both negative mean PDO and lower monthly average temperatures. A strong correlation was found between a period of dramatic decline in False Bay eelgrass (2015 to 2017), and both higher average monthly temperatures and an atypical PDO positive phase. Analysis of historic eelgrass cover also revealed persistent patches of eelgrass consistent since 1990. These persistent patches deemed 'elder patches', show eelgrass beds within False Bay that have remained unchanged in expanse for over thirty years.

1.0 Introduction

False Bay is located on San Juan Island in the San Juan Archipelago of northwest Washington state. False Bay covers approximately 100 hectares and can be described as a predominately shallow mudflat with a rich biodiversity. Within False Bay's deeper intertidal and shallow subtidal zones exist multiple eelgrass *(Zostera marina*) beds each forming their own microhabitat. Eelgrass is a seagrass species native to the Northern Hemisphere which supports productive estuarine and coastal habitats throughout the Salish Sea. It provides important refuges for organisms, contributes to primary production, and facilitates nutrient cycling. A diverse and abundant array of organisms live within or utilize these undersea meadows in the Pacific Northwest including anemones, mollusks, crustaceans, fish, and sea birds (Phillips 1984**)**. Eelgrass beds also provide habitat for species harvested by commercial and native fisheries including Dungeness crab (*Cancer magister*), Pacific herring (*Clupea pallasii*), juvenile coho (*Osteichthyes kisutch*), and chinook salmon (*O. tshawytsch*a) (Phillips 1984; Waycott et al. 2009**)**.

Extensive eelgrass meadows within the Salish Sea have important roles not only in the life cycles of these organisms, but also on the people who rely on them. For instance, eelgrass was important to coast Salish People including the Kwakwaka'wakw, a modern population in the Discovery Islands of British Columbia Canada. Ts'áts'ayem, the Kwak'wala word for eelgrass, was an important traditional source of food during the springtime due to its rare sucrose content only otherwise available in fruit/berries, inner tree bark, and marsh root vegetables (Lieberman 2003; Cullis-Suzuki et al. 2015). Furthermore, salmonids and Pacific herring, which are cultural keystone species for Alaska natives, rely on eelgrass meadows for nurseries (Moss 2016).

Currently, global eelgrass abundance is declining for a multitude of reasons, many of which are associated with climate change (Ehlers et al. 2008; Unsworth et al. 2015; Groner et al. 2016; Walker et al. 2019). Losses or changes in seagrass meadows commonly correlate with eutrophication, increases in sedimentation, decreases in light availability, and direct physical disturbances such as severe storms (Waycott et al. 2009; Unsworth 2015). Eelgrass meadows and their paired ecosystems have also been shown to be negatively affected by increasingly extreme summer temperatures (Ehlers et al. 2008). Continuous water-surface temperatures over 25°C have consistently caused eelgrass decline or die-off in both lab and field conditions and as global surface temperatures continue to rise, eelgrass meadows and their associated organisms may suffer (Ehlers et al. 2008; Unsworth et al. 2015). Eelgrass patches with lower genotypic diversity are known to have reduced shoot density when exposed to temperature extremes (Ehlers et al. 2008). Thus, genotypic diversity allows for niche organisms within populations to withstand environmental stressors, including those associated with climate change. Smaller populations of eelgrass, such as those in False Bay, may be at greater climate associated risk due to lower genetic diversity, greater desiccation, and susceptibility to storms.

Global air temperatures continue to rise with predictions for the end of the current century as high as 4.8°C more than the previous century (Walker et al. 2019). Washington state recorded its highest temperatures in the summer 2021 with a record of 108°F on June 28th (NCEI 2021). Another threat to global seagrass extent is the threat of eelgrass wasting disease caused by *Labyrinthula* spp. (Groner et al. 2016). Eelgrass wasting disease is hypothesized to correlate with immunosuppression-paired environmental stressors such as temperature increase (Groner et al. 2016; Sullivan et al. 2018). Considering eelgrass' important role as an ecosystem engineer and

its contributions to humanity, understanding both its current and historical distribution is a primary prerequisite to conservation and management of seagrass resources.

Using techniques utilizing more sophisticated satellite imagery and analysis, modern cartography allows for a greater identification of coastal resources than previously possible (Meehan et al. 2005; Short et al. 2008). Cartography is a useful tool to portray species composition, meadow distribution, and abundance when illustrating seagrass beds. Generated maps can illustrate a diverse array of concepts including large scales, presence/absence, and changes over time (Meehan et al. 2005; Short et al. 2008; Traganos et al. 2018). Understanding temporal changes in seagrass meadows requires historical data such as aerial imagery which can be especially advantageous for mapping dense seagrass meadows in temperate regions with lower turbidity (Short et al. 2008). Seagrass cover quantified using aerial photos must be digitized and rectified to be accurate at a scale of 1:10,000 in order to generate an acceptable map (Short et al. 2008). Large scale maps with lower resolution require less sampling intensity and often utilize statistical extrapolation. However, to monitor finer details such as change in seagrass cover over time, more precision is required.

In order to obtain more localized data, greater sampling intensity with increased precision is required to provide levels of detectable change. Mapping seagrass meadows and other features of marine habitats through aerial photography brings many difficulties affecting precision (Meehan et al. 2005; Short et al. 2008). These challenges include blue light penetration at depths greater than 3m, sun reflection, turbidity plumes, and sea surface conditions. Furthermore, remote sensing is not always effective or possible due to tidal stages or low-resolution aerial imagery. Thus, aerial photography alone is not sufficient to illustrate temporal change in seagrass extent. Ground truthing (or field observation) serves to examine areas where imagery does not

provide sufficient information and to reference information for accuracy assessment. Mapping accuracy is classed as either thematic or spatial. Thematic accuracy is a determination of the correctness of the features identified on the map product covering whether a patch of seagrass was correctly labeled as seagrass in the map, or it was incorrectly labeled as algae (or vice versa) (Short et al. 2008). Spatial accuracy is a measure of the positional correctness of boundaries and features in a map product (Short et al. 2008). Both levels of accuracy are critical to create a map worthy of analysis.

False Bay serves as an opportunity to test methodology for measuring eelgrass extent in a previously unquantified area. This project mapped and calculated changes over time in observable eelgrass abundance within the bay. Correlations with air temperature and Pacific decadal oscillation were also explored to link eelgrass changes and possible contributing factors. Additionally, this study aimed to create a preliminary data set for future studies involving False Bay eelgrass.

2.0 Methods

The primary objective of these methods was to establish a dataset portraying changes in observed eelgrass within False Bay Washington. Methods are divided into four different sections to better describe individual processes used to produce results. First, field surveying describes all work done in False Bay to verify observations made from aerial imagery. Second, spatial data and imagery explain work done in ArcGIS to quantify areas of eelgrass meadows, both modern and historic, in the shallow subtidal zone of False Bay. Third, spatial analysis describes work done in ArcGIS layering eelgrass polygons derived from previous sections to quantify changes over the entire study period (1990-2021). Lastly, Climate data describes work done to transform

NCEI temperature and PDO data to be used in analysis exploring possible contributing factors to eelgrass changes.

2.1 Field Surveying

Drone imagery showing eelgrass extent at neap tide during the Summertime of 2021 was analyzed. The largest eelgrass beds within the shallow subtidal zone were identified from this imagery and selected for field observations. Field observations were used to verify perceived eelgrass beds and expand available False Bay eelgrass data and will be referred to as ground truthing. Ground-truthing was established by snorkeling with short underwater dives in combination with a floating GPS device (Garmin eTrex10).

During data collection, the GPS was used to record the perimeter of eelgrass beds using the 'track manager' feature and the location of smaller beds using waypoints. Snorkelers ground truthed the perimeter of shallow water False Bay eelgrass meadows in the field with a floating GPS unit. Deeper water areas proved more challenging to ground truth where freediving was required in addition to surface snorkeling to validate eelgrass perimeters. Waypoints from multiple surveys were recorded in meaningful spots where bed shapes could be later constructed from the points.

Abundance was also recorded through shoot density measurements. Shoot density was estimated onsite by hand using a submersible $0.25m^2$ quadrat. The quadrat was placed underwater on the sediment, GPS coordinates were recorded on the surface above the quadrat, and shoots were counted. Special attention was also brought to a 100 meter transect on the Northwestern edge of False Bay (see Fig. 6) which contains previous shoot density counts from 2005-2014. This was achieved through the setup of an underwater transect and shoot density

counts at previously recorded meter marks. The underwater transect was placed by swimming both ends to marked coordinates and weighing it down with rocks. Modern shoot density counts were compiled and averaged into the same format as preexisting transect shoot density data. Averaged annual transect data was coupled with historic data in table format (Fig. 6)

2.2 Spatial Data and Imagery

Aerial imagery of False Bay was acquired through the Washington Department of Ecology website and Google Earth Engine Data Catalog (GEE). Due to large differences in photo angle, images obtained from the Washington Department of Ecology were not used in spatial computations. This decision was made in order to ensure precision in photo scale and resolution during spatial analysis. Aerial photography, satellite imagery, GPS, ground truthing, and GIS were all used to determine the extent and area of seagrass meadows in False Bay both modern and historic.

Nine historic images in total were collected with original captures in the years 1990, 2005, 2006, 2009, 2011, 2014, 2015, 2017, and 2018. Each individual image acquired from GEE differed in year but had identical scale and spatial location. This allowed for identical georeferencing of each individual image within ArcGIS in which the first image was used as the primary reference sharing control points with all others. Errors in spatial data occurring in the primary reference image, are shared among all georeferenced images in the study period. This ensured that any spatial variance in eelgrass area resulting from georeferencing, is equal among all ArcGIS polygons created. Thus, georeferencing transformation distortions on observed eelgrass patches are equal among all years analyzed.

Each individual image was both independently analyzed and referenced to other images to verify rock features or shadows. Specifically, this comparative method was used when identifying Western and Northern eelgrass patches due to high accumulations of Ulva and a greater number of shadows. Furthermore, Washington Department of Natural Resources (WADNR) transect data from the Submerged Vegetation Monitoring program directly overlapped with analyzed 2009 imagery (WADNR 2020) (see Fig. 7). Washington DNR data present from 2004 was also utilized for ground truthing of available 2005 imagery. Ground truthing was also established by the historic shoot density data acquired from the previously mentioned transect (see Fig. 6&7).

Collected GPS data sets from field surveys were first exported to Garmin Basecamp, converted to '.gpx' file format, and imported into ArcGIS Pro. GPS waypoints were converted into point data within ArcGIS Pro. Recorded eelgrass perimeters from field surveying were converted into shapefiles to be used as spatial references while tracing the most recent satellite imagery. GPS perimeters included extraneous data points at the start and end of recordings correlated to time periods spent stationary in the water using the GPS. However, these extra points were easily identifiable as they were sequenced and in close proximity to each other. Extraneous data points were removed from visual layers using layer definition queries. Areas observed in the aerial imagery perceived to be eelgrass were traced and exported as polygons within ArcGIS Pro. Aforementioned GPS perimeters were used as ground truthing references in all traces. This not only provided data validation but also support when indistinguishable dark signatures such as shadows/rocks hindered tracing. Tracing scale emulated Meehan et al. 2005 in which all images were enlarged on-screen to a scale of 1:1000 for consistency and seagrass

extent was traced on-screen using a mouse. Darker areas in the marine environment perceived to be eelgrass were traced and exported as polygons within ArcGIS for area analysis.

2.3 Spatial Analysis

Both modern and historic eelgrass traces were recorded as polygon shapefiles within ArcGIS Pro. Eelgrass meadow polygons created within ArcGIS were overlaid over previous annual eelgrass layers to analyze changes in eelgrass extent. Using the ArcGIS 'intersect' tool, different map layers were created to show areas where eelgrass has remained unchanged, disappeared, and fluctuated throughout different time periods. Before area calculations were made, all shapefiles were converted into raster grids (grid size = $1ft^2$) and collectively overlaid for analysis. Because polygon shapefiles record area in fractions of a pixel and raster grids convert to whole values, raster grid areas were negligibly different than original traces (mean difference = $1.7m^2$). These eelgrass raster grids were reclassified with numerical values indicating presence/absence or associated with their respective year. This allowed for raster calculations to be made showing permanence (Fig. 3) and yearly changes (Fig. 1). Presence absence raster grids had numerical values of 1 indicating presence and 0 for absence. Thus, performing raster additions of two raster grids would yield a value of 2 for areas of permanence, 1 for areas of gain/loss, and 0 for absence. The individual areas of these categories were reported within ArcGIS as grid counts and later converted into square meters. This concept was expanded to find the area of eelgrass extent growth/loss between studied periods (see Fig.1), as well as the permanence of patches (see Fig. 3). Year specific calculations were done in a similar manner using unique values associated with each year.

2.4 Climate Data

In order to investigate possible contributing factors to variance in False Bay eelgrass extent, climate data was obtained from the National Oceanic and Atmospheric Administration's National Center for Environmental Information (NCEI 2021). This data local to San Juan County was processed within RStudio to display air temperature data specific to Friday Harbor airport; the nearest site to False Bay (see Fig. 2). Temperature data was transformed into monthly averages from recorded daily maximums. Pacific Decadal Oscillation (PDO) data was also retrieved from NCEI and transformed within RStudio to obtain annual mean values. 2021 PDO data lacked October, November, and December values during calculations, resulting in a more positive annual mean PDO value than expected (still highly negative). RStudio packages used to transform both temperature and PDO data were 'dplyr', 'lubridate', and 'ggplot2'. Average monthly air temperatures, mean annual PDO values, and False Bay eelgrass areas were grouped by year (see Fig. 2). Due to a complete lack of eelgrass area data from 1991-2004, climate data was clipped to display 2005-2021 rather than the entire study period.

3.0 Results

According to Short et al. 2008, only one observation is necessary at a ground truth site but should also include measurements of abundance, and species composition. Since *Z. marina* was the only species of seagrass observed in the field, species composition was not recorded past initial surveys. Areas of eelgrass beds within the intertidal/higher subtidal zone of False Bay were derived from aerial imagery analyses and verified (ground truthed) via field surveys and historical data. The calculated area of 2021 eelgrass beds within the intertidal/higher subtidal zone of False Bay was $10583m^2$. The first year of analysis, 1990, was the minimum value of recorded eelgrass area within the data set spanning $8317m^2$. The maximum value of recorded eelgrass area was $16120m^2$ in 2014. Overall, the data shows an overall increase of $2266m^2$ of

eelgrass within False Bay from 1990-2021. However, this is an overall change and not a steady slope of increase as many years saw decreases in area of eelgrass extent from previous years analyzed (see Fig.1). In addition to changes in extent, persistence of eelgrass beds was also determined through spatial analysis. Modern (2021) eelgrass beds within the shallow subtidal zone were able to be dated by aerial imagery. The oldest expanses of observed eelgrass persist through the entire study period of 1990-2021 (see Fig.5).

Transformed climate data reveals changes in both mean Pacific decadal oscillation and average air temperatures over the study period (see Fig. 2). PDO in years 2014,2015, and 2016 is positive in contrast to all other years quantified in the dataset. All other years outside the positive phase in PDO are negative values ranging from -0.10 to -1.81. Average monthly temperature maximums also show variance within the study period. During the 2009-2014, July of 2009 had an average max air temperature of 23.5℃, followed by lower average summer temperatures (July of 2010: 21.8℃, 2011: 20.7℃, 2012: 20.1℃, 2013: 22.52℃). Summertime temperature averages from 2015-2018 were recorded to be greater than those in preceding/following years. Average maximum July air temperatures from 2015-2018 measure 24.8, 22.8, 22.9, and 25.6℃ respectively. Correlations between temperature, PDO, and eelgrass extent are explored in the discussion.

4.0 Discussion

I hypothesized False Bay eelgrass was steadily decreasing due to rising global temperatures. In fact, our study demonstrates that eelgrass has slightly increased since both 1990 and 2005. Rather than strictly decreasing in direct correlation to rising global temperatures, eelgrass extent appears to fluctuate with Pacific Decadal oscillation as well as maximum summer temperatures. Rather than a flat decrease, there are multiple periods of variable change

throughout the study period. Phases of relative stability (2005-2009), expansion (2009-2015), and rapid reductions (2015-2017) are all shown within the data set (Fig. 1).

Within the study period of 1990-2021, calculations show three periods of eelgrass expansion (g1:1990-2005, g2:2006-2014, and g3:2018-2021), and two periods of eelgrass decline (d1:2005-2006, d2:2014-2018). The longer period of decline, d2, shows an overall reduction in the area of eelgrass extent by $7168m^2$. Majority of d2 eelgrass reduction (-$7069m^2$) occurred between the 2015/2017 years of analysis. The largest period of eelgrass expansion, g2, shows an overall increase in the area of eelgrass extent by $7575m^2$ with the largest increase (+$5534m^2$) occurring between the 2009/2011 years of analysis. All area changes between years analyzed can be seen in Figure 1 and cumulative changes can be seen in Figure 4.

There appears to be a correlation between the intensity and direction of the Pacific decadal oscillation, air temperature, and area of eelgrass extent within False Bay (see Fig. 2). Anomalously warm sea surface temperatures along the Pacific Coast correspond to PDO in a positive phase/having a positive value (Manuta & Hare 2002; NCEI 2021). In contrast, cool sea surface temperatures in North American coastal waters follow negative PDO values (Manuta & Hare 2002; NCEI 2021). Thus, negative PDO values may be correlated with cooler water temperatures and positive a PDO with warmer temperatures around the San Juan islands and within False Bay.

When analyzing mean annual PDO values in relation to change in eelgrass extent, consistent negative phase PDO values correlate to increases in False Bay eelgrass. The largest period of eelgrass expansion (g2:2009-2014) occurs during the longest and most extreme negative phase in PDO. As PDO moves from negative to positive phase (2013-2014), eelgrass expansion appears to slow from 2011-2014. Years of eelgrass decline (2014, 2015, 2017)

correspond to this period of positive PDO phase (2014-2016) and a near zero value (-0.09) in 2017. Unfortunately, 2016 lacked proper imagery for area extent analysis. If eelgrass data could be obtained in the future through another source, this correlation could be further analyzed to see if majority of eelgrass reductions occurred from 2015-2016 when PDO was most positive and sea surface temperatures warmest. Eelgrass expansion from 2018-2021 also occurs in tandem with a negative mean annual PDO values.

Relationships can also be observed between average monthly air temperatures and False Bay eelgrass extent (Fig 2). During the 2009-2014 expansion period, July of 2009 had a relatively higher average max air temperature of (23.5℃), followed by lower average summer temperatures (as much as -3.4℃) from 2010-2013. Thus, as summer temperatures cooled, eelgrass expansion occurred. Following this period of growth average extreme temperatures rise in tandem with large eelgrass reductions (d2 period). These temperatures approach lab conditions (25.0℃) mentioned in Ehlers et al. 2008 which caused eelgrass decline and die off. Considering temperature data was calculated as averages, many days with temperature maximums greater than 25.0℃ likely occurred. Thus, eelgrass exposure to these proven hazardous temperatures is likely considering predictably low summertime tides. Following d2, eelgrass expansion occurs from 2018-2021 correlating with average maximum summer temperatures less than 22.5℃. Temperatures were missing from acquired NCEI data including May 2020, June 2015, and September 2014. July was chosen to discuss correlations due to its extreme values and complete data set. Further statistical analysis in the future could be beneficial to test the lag time between PDO/temperature fluctuations and eelgrass responses.

During spatial analysis of eelgrass persistence, areas of highly persistent patches of eelgrass deemed ‘elder patches’ were identified. Elder patches were grouped in two different

categories; areas of eelgrass observed in all years (elder-1990), and areas of eelgrass observed 2005-2021 (elder-2005) (see Fig. 5). Cumulative area of all 2005 elder patches is $761m^2$ and 1990 elder patches is $160m^2$. Two elder patches belonging to elder-2005 makeup the majority of area; the largest occurring in a central meadow ($495m^2$) and the second in the westernmost bed ($180m^2$). The largest of the 1990 elder patches occur within these two 2005 elder patches measuring $84m^2$ in the northern bed, $16m^2$ and $52m^2$ in the central meadow. Elder-2005 and elder-1990 represent approximately 7 and 1.5% respectively of total quantified 2021 eelgrass extent.

Throughout the study period, different expanses of eelgrass have emerged, changed, or disappeared. During the same year, specific areas of eelgrass may decline while others expand. Cumulative eelgrass area observed in the entire study period is greater than the modern extent of eelgrass within False Bay but that does not mean eelgrass is declining (see Fig 4). Excluding the elder patches, this False Bay eelgrass appears highly variable not only in eelgrass extent but in density. Observation of shoot density counts conducted between 2005-2014 show great variations in mean shoot density between single years (see Fig. 6). Given that these counts were conducted during the same time period each year, the data shows variance in abundance among each individual year. Modern shoot density data collected during this study (2021 value) may be greatly skewed due to differing techniques (underwater counts vs terrestrial counts) and time of collection (summer vs autumn). Rather than specific eelgrass beds or individual eelgrass meadows, False Bay can be viewed as a seagrass zone

The discovery of elder patches within False Bay highlights the idea of a seagrass zone. If an eelgrass meadow is a forest, then these elder patches are the old growth. The choice to split the elder patches into two categories was made for two reasons. First, the gap between 1990 and

2005 is equal in duration to the rest of the study window (2005-2021) with only two reference images rather than nine. Second, eelgrass meadows observed in 1990 show more spatial differences than the rest of the data set. Thus, the inclusion of two categories of elder patches seeks to include all available data (elder-1990) and highlight the shape and continuance of these persistent patches (elder-2005). The elder patches of False Bay bring forth further questions and future opportunities for study.

The largest of all the elder patches is in the central eelgrass meadow within the high subtidal/intertidal zone (see Fig 5). This elder patch spanning approximately $500m^2$ is surrounded by the largest extent of observed continuous eelgrass within False Bay. Through PDO anomalies and extreme weather events, this area of the seagrass zone has remained unchanged since 2005. This elder patch could represent a genetically distinct patch of eelgrass optimally adapted to the False Bay habitat, or a physical area best suited to foster eelgrass. The existence of this highly persistent eelgrass demonstrates the resilience of False Bay eelgrass. This eelgrass resilience is the capacity to absorb repeated disturbances and ability to adapt to change without shifting to an alternative state of stability (Holling 1973; Unsworth et al. 2015). As other portions of this eelgrass zone have declined or expanded, this elder patch has proven highly resilient. Furthermore, there may be more elder patches within False Bay in the deeper subtidal zones, however they were not able to be sufficiently quantified using techniques used in this study.

4.1 Future Research

Questions arise about the specific portion of the bay the largest elder patch inhabits as well as the individual plants within it. An important question to be answered involving the elder patches is the reason why this $500m^2$ portion of the bay has proven optimal for eelgrass.

Initially, analysis could be conducted to help narrow the possibilities to physical or genetic origins. Physical analysis could involve sediment/carbon analysis or hydrodynamics. Cores could be taken from areas inside and outside the elder patches for comparative analysis. Furthermore, genetic analysis beyond the scope of this project could attempt to answer whether the elder patches involve individual plants with quantifiable genetic variances.

Questions also remain involving deeper subtidal eelgrass beds in False Bay. Washington DNR seagrass data includes deep water transects from 2003, 2004, and 2009 illustrating eelgrass. Those transects could be repeated and translated to show variance in subtidal eelgrass and its relation to intertidal/high subtidal zone eelgrass changes quantified in this study. Maps and figures generated from further subtidal studies could be correlated with the same climate data used for shallow subtidal patch correlations. Furthermore, the patterns observed in False Bay eelgrass could also be expanded and compared to other sites. Perhaps False Bay eelgrass shows patterns consistent to other sites seen at local or even global levels.

Acknowledgements: I would like to acknowledge my professors Dr. Brooke Sullivan, Dr. Wendell Raymond, and Dr. Megan Dethier for their insights, comments, and instruction. Seagrass expert Dr. Sandy Wyllie-Echeverria for their enormous help and support with connections, references, and anything eelgrass related. Marc Santos for their brilliant GIS tips as well as Sadie Trush. Dr. Drew Harvell for providing drone imagery and Olivia Graham for further supporting eelgrass imagery. Dr. Bart Christiansen with the Washington DNR and Pema Kitaeff, Friday Harbor Labs dive expert and snorkel provisioner. I would also like to acknowledge the generous funding from the Mary Gates Endowment. A special thank you to the entire BMEE class including Dr. Alan Trimble as well as Maddie Byrne and Kevin Penny for their invaluable comments and company.

Figures

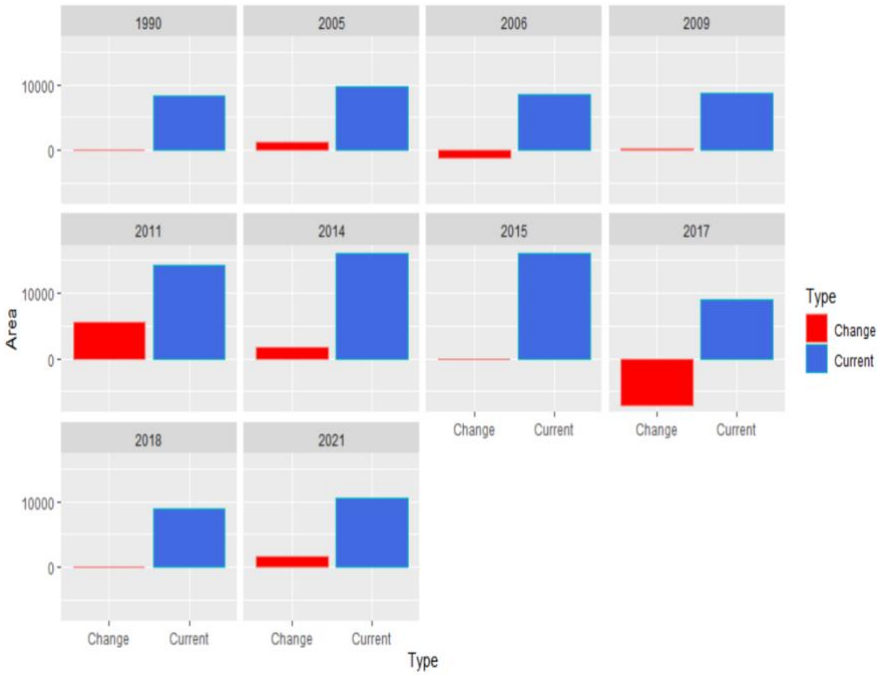

Year	Current(m^2)	Change(m^2)
1990	8317	0
2005	9626	1309
2006	8545	-1081
2009	8741	196
2011	14276	5534
2014	16120	1845
2015	16044	-77
2017	8975	-7069
2018	8953	-22
2021	10583	1631

Figure 1. Temporal change in False Bay eelgrass: Area in square meters of eelgrass from ten different years in the period of 1990-2021. Area of perceived eelgrass meadows is displayed in blue as 'current'. Reduction/growth in eelgrass in relation to the previous year analyzed is displayed in red as 'change'. Years of overall reduction in eelgrass extent show change bars extending negatively in magnitude below the current area values.

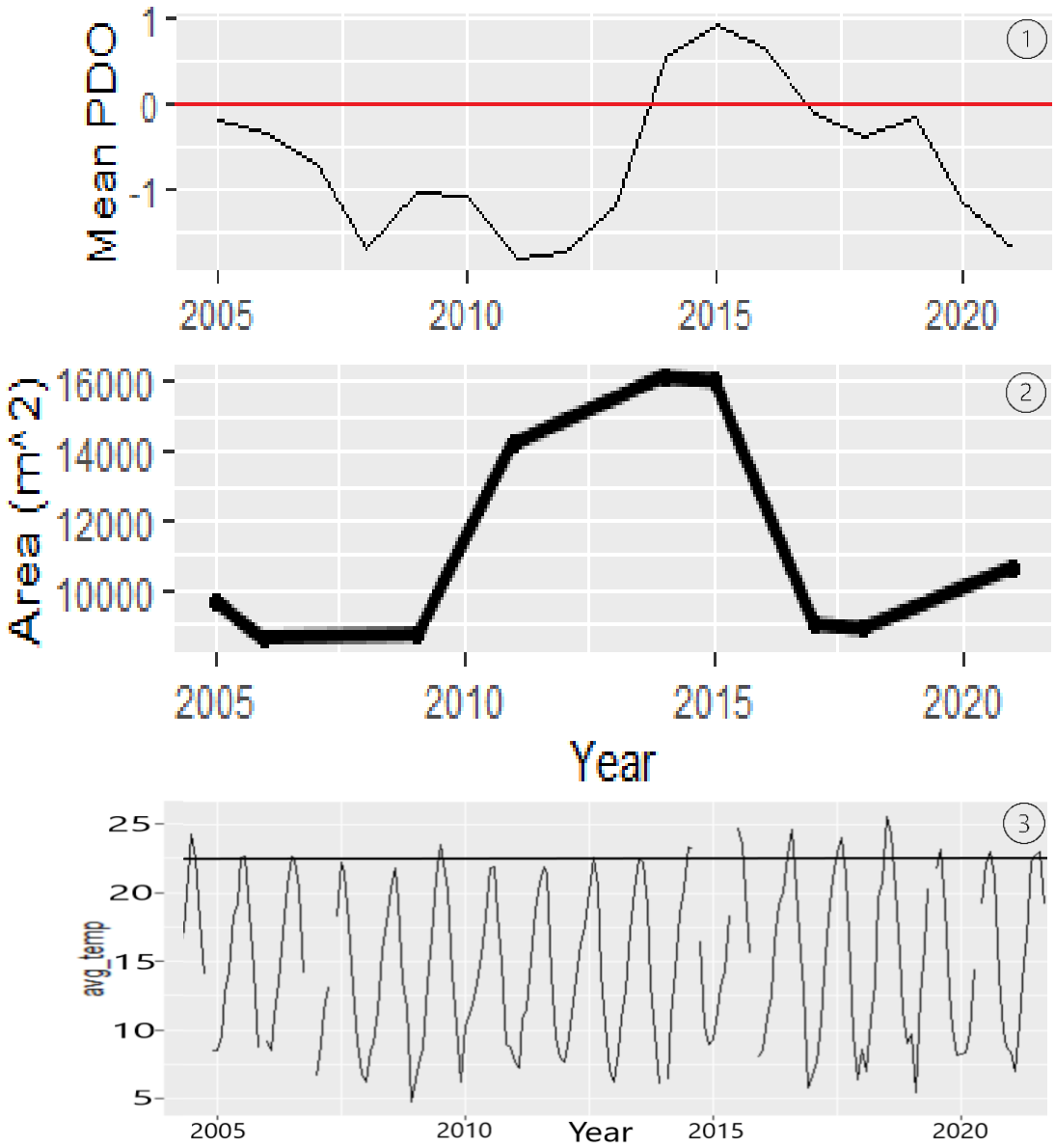

Figure 2. Observed correlations between PDO, air temperature, and eelgrass extent: All graphs span the same yearly range of 2005 – 2021. Graphs 1 and 3 use data obtained from NCEI while graph 2 contains data collected from this study. **(1)** Top graph displays mean annual values for Pacific Decadal Oscillation index. **(2)** Middle graph displays area of eelgrass visible meadows calculated from GIS raster data. Numerical values can also be seen in figure 1. **(3)** Displays average monthly air temperature collected at Friday Harbor airport weather station. The horizontal line is drawn at 22.5 degrees Celsius. Gaps in the line graph represent data missing from NCEI collected source.

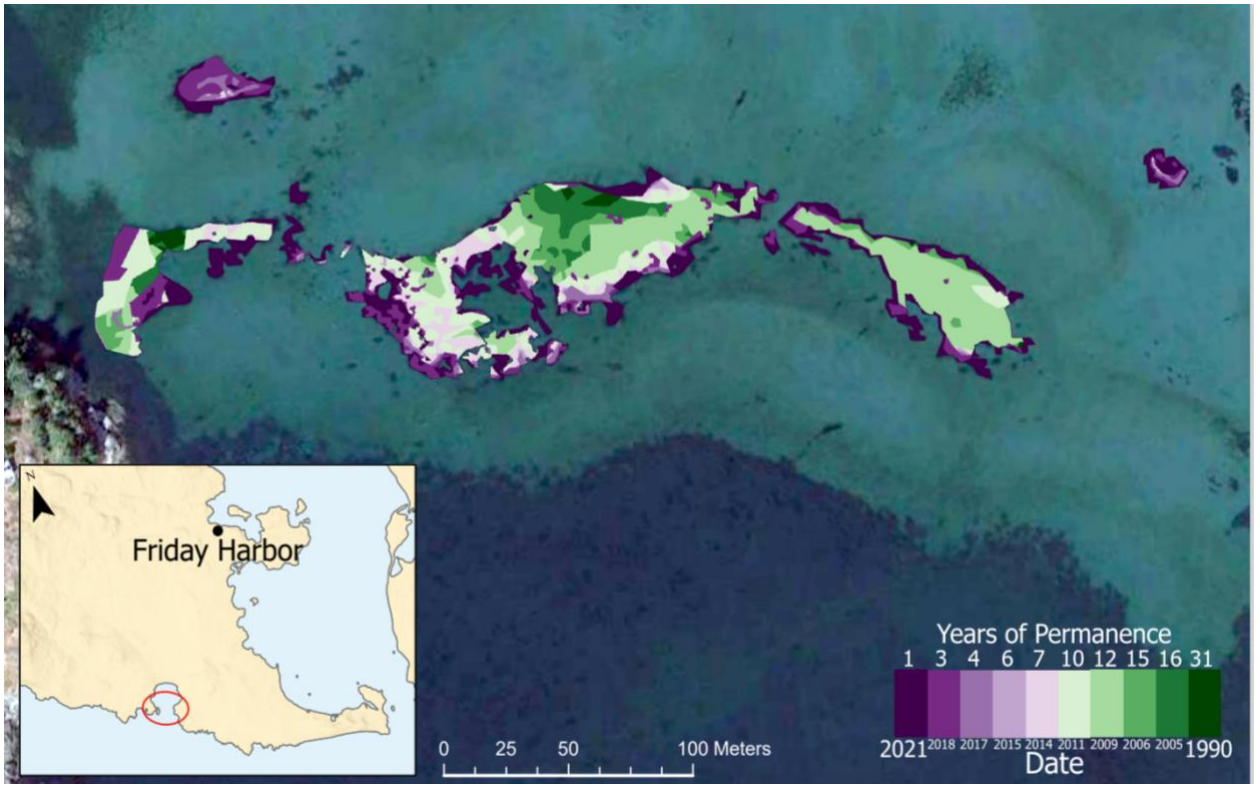

Figure 3. Permanance of eelgrass beds: False Bay eelgrass beds in 2021 within intertidal and high subtidal zones eelgrass is filtered by years of permanence. Permanance in this figure is defined as the amount of sequential years in which eelgrass was observed. Date displays the earliest quantified year in which eelgrass was detected within available imagery. Purple areas correspond to areas where eelgrass more recently emerged while green areas represent areas of more persistant eelgrass. All areas of eelgrass meadows represented within the figure exist in 2021. The areas of highest permanence (elder patches) are further displayed in figure 5.

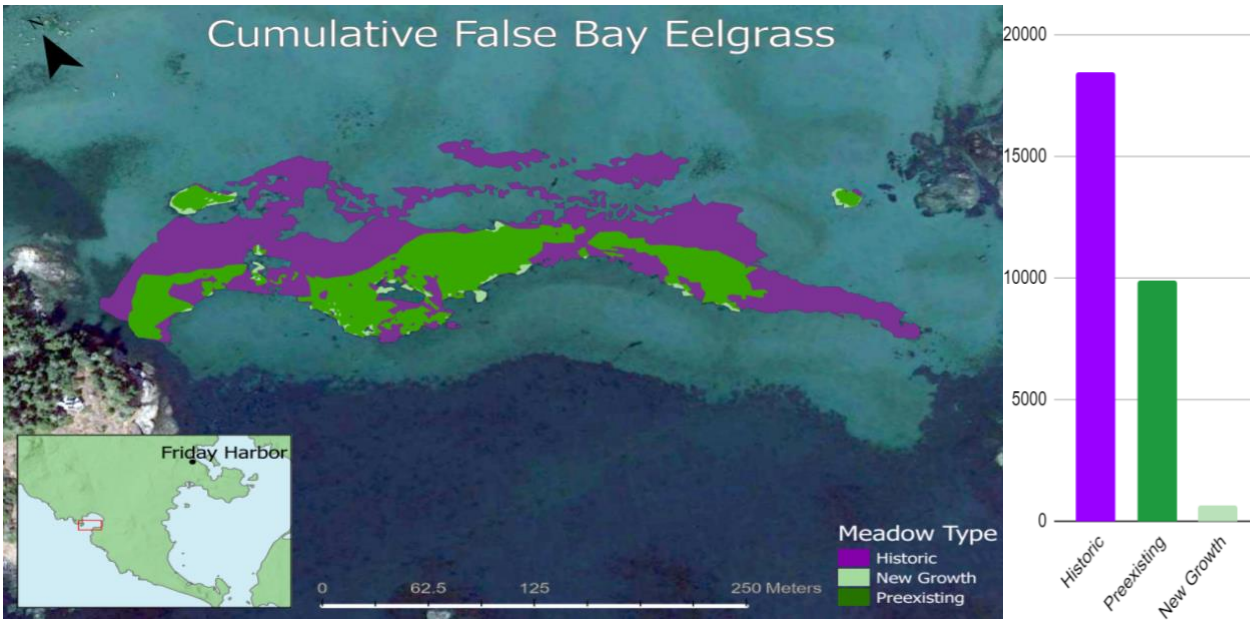

Figure 4 Cumulative Observed Eelgrass: Eelgrass meadows of different types are displayed. Historic meadows correspond to areas in which eelgrass was observed 1990-2018 and is no longer present. Preexisting meadows refer to areas of eelgrass present in 2021 which have persisted from previous years. New growth meadows represent eelgrass beds unique to 2021 imagery analyzed. Graph displays area of each meadow in square meters.

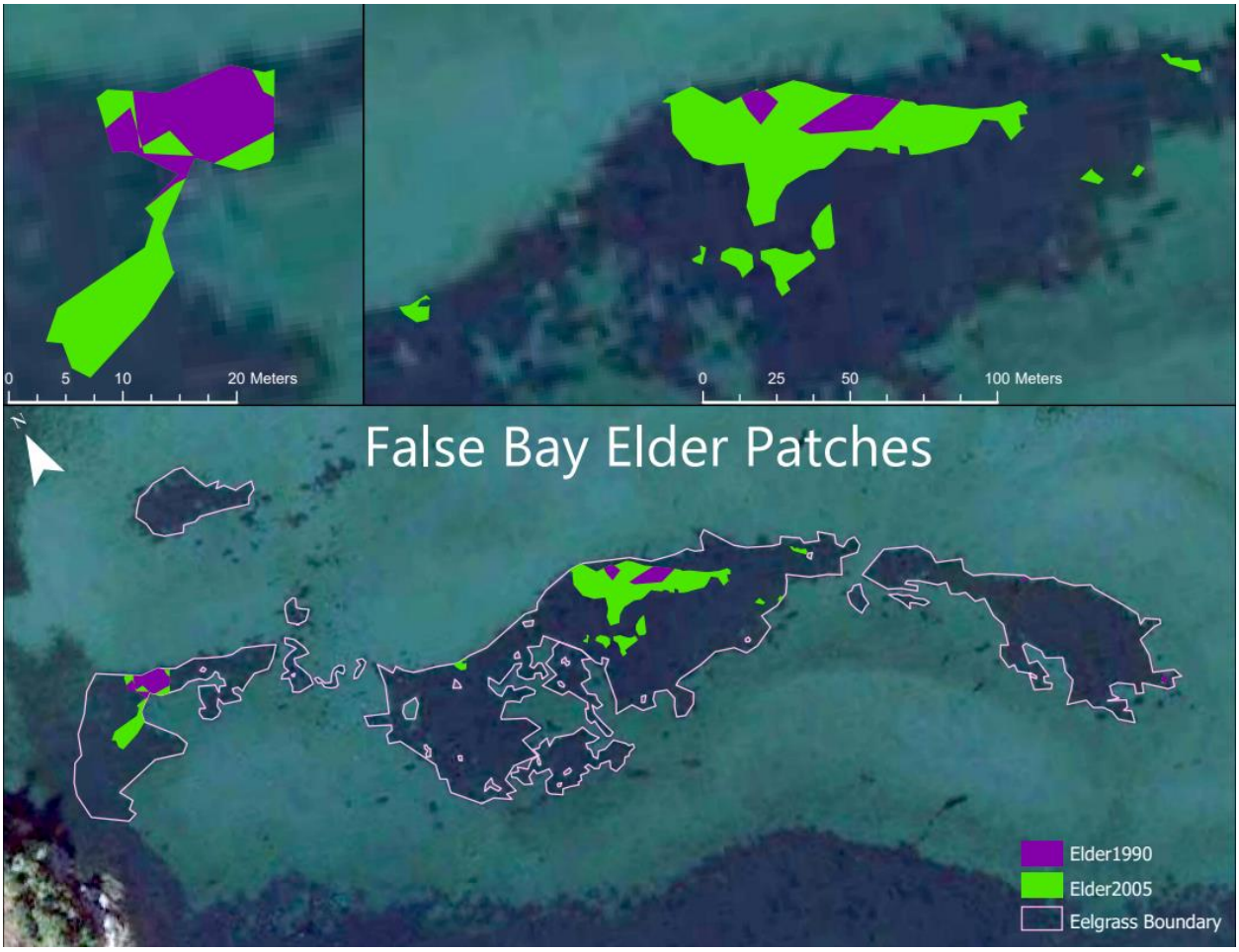

Figure 5. Elder Patches of False Bay: Eelgrass beds of highest persistence are shown. Eelgrass boundary represents the extent of all quantified eelgrass present in 2021 during the study. Elder1990 represents eelgrass beds which have persisted for 31 years (1990-2021). Elder2005 represents eelgrass beds which have persisted for 16 years (2005-2021). Images in the top row are zoomed in on the largest of the two elder patches. Area of largest elder patches is given in results (pg. 14). Areas of largest Elder2005 patches are 495m^2 (top right image) and 180m^2 (top left image). Areas of largest Elder-1990 patches are 84m^2 (top left),16m^2 and 52m^2 (top right image).

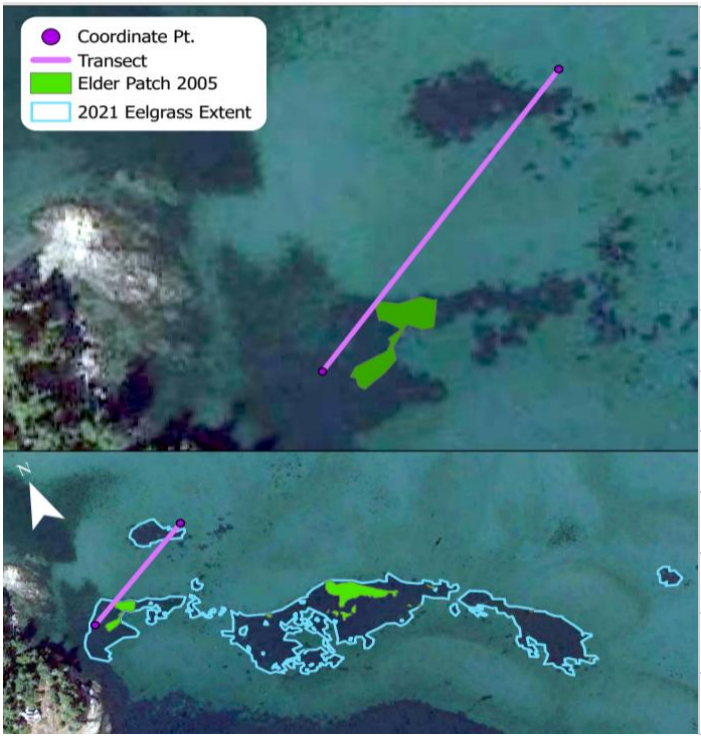

Year	Mean Shoot Density
2005	13.2
2006	11.7
2007	6.1
2008	11.4
2009	6.5
2010	15.8
2011	4.6
2012	16
2013	20.1
2014	9.2
2021	2.3

Figure 6. Shoot density counts at transect: Location of transect is shown in relation to modern eelgrass extent and 2005 elder patches. Shoot density counts collected prior to this study (table values 2005-2014) are combined with collected 2021 data. Coordinate points (48.48275N, 123.07415W & 48.483267N, 123.072967W) are shown where end points of a 100 meter transect were laid. Means shoot densities are the result of 10 randomly selected points on the 100m transect hand counted using a 0.25m^2 quadrat.

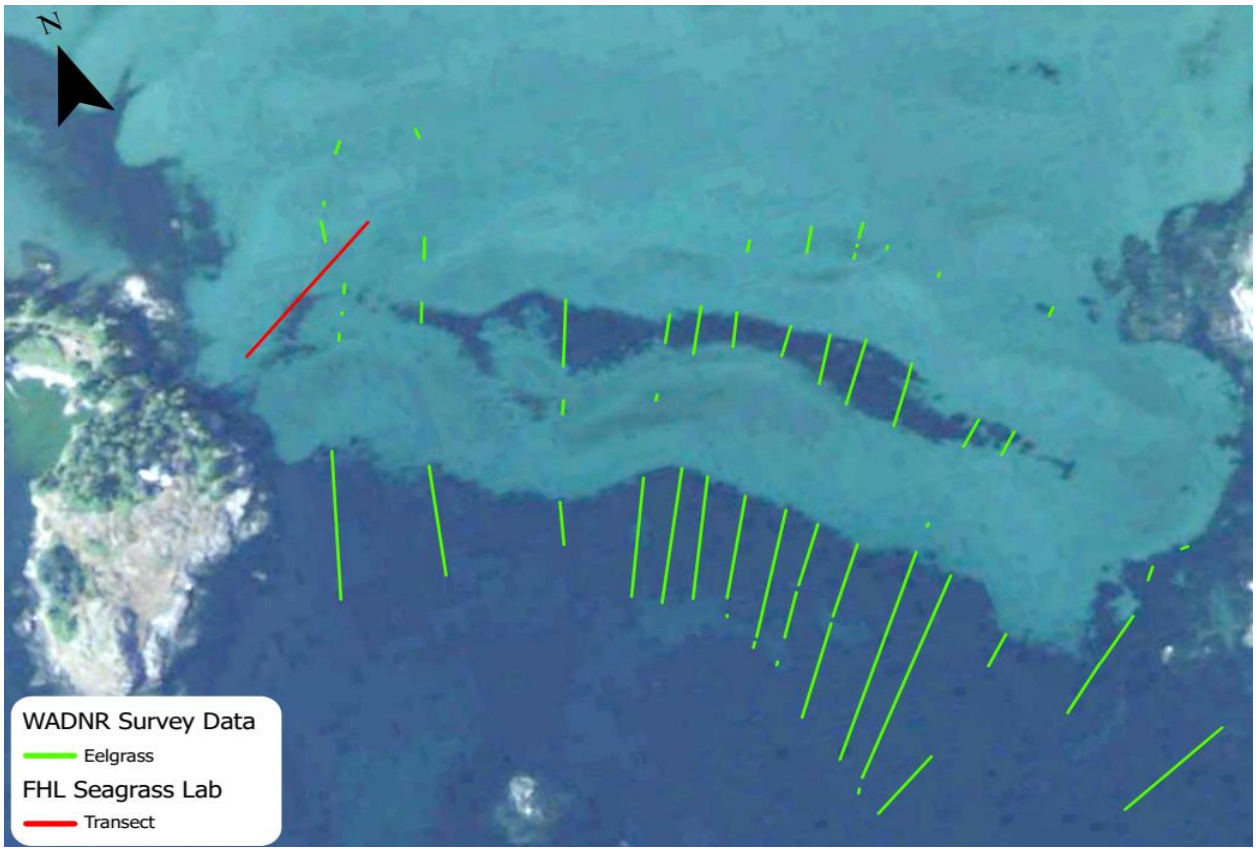

Figure 7. Ground truthing historic imagery: Different data sets are displayed which were used to validate eelgrass expanse within older aerial imagery. Washington Department of Natural Resources data is displayed in green. This data is in the form of underwater camera tows translated into presence absence transects. The transect used in shoot density counts conducted by FHL Seagrass Lab is shown in red. Both of these datasets are overlaid 2009 False Bay imagery in which both sets have data for 2009.

References

Cullis-Suzuki S, Wyllie-Echeverria S, Dick KA, Sewid-Smith MLD, Recalma-Clutesi OK, & Turner NJ (2015). Tending the meadows of the sea: A disturbance experiment based on traditional indigenous harvesting of Zostera marina L. (Zosteraceae) the Southern Region of Canada's West Coast. *Aquatic Botany*, *127*, 26–34. https://doi.org/10.1016/j.aquabot.2015.07.001

Ehlers A, Worm B, & Reusch TBH. (2008). Importance of genetic diversity in Eelgrass Zostera marina for its resilience to Global Warming. *Marine Ecology Progress Series*, *355*, 1–7. https://doi.org/10.3354/meps07369

Groner ML, Burge CA, Kim CJ, Rees E, Van Alstyne KL, Yang S, Wyllie-Echeverria S, Harvell CD. Plant characteristics associated with widespread variation in eelgrass wasting disease. Dis Aquat Organ. 2016 Feb 25;118(2):159-68. doi: 10.3354/dao02962.

Hayduk JL, Hacker SD, Henderson JS, & Tomas F (2019). Evidence for regional-scale controls on eelgrass (*Zostera marina*) and Mesograzer community structure in upwelling-influenced estuaries. *Limnology and Oceanography*, *64*(3), 1120–1134. https://doi.org/10.1002/lno.11102

Holling CS (1973). Resilience and stability of Ecological Systems. *Annual Review of Ecology and Systematics*, *4*(1), 1–23. https://doi.org/10.1146/annurev.es.04.110173.000245

Lieberman LS (2003). Dietary, evolutionary, and modernizing influences on the prevalence of type 2 diabetes. Annu. Rev. Nutr. 23, 345–377.

Manuta NJ & Hare SR (2002). The Pacific Decadal Oscillation. *Journal of Oceanography*, *58*, 35–44.

Meehan AJ, Williams RJ, & Watford FA (2005). Detecting trends in seagrass abundance using aerial photograph interpretation: Problems arising with the evolution of mapping methods. *Estuaries*, *28*(3), 462–472. https://doi.org/10.1007/bf02693927

Moss ML (2016). *The nutritional value of Pacific herring: An ancient cultural keystone species on the Northwest Coast of North America*. Journal of Archaeological Science: Reports, 5, 649–655. https://doi.org/10.1016/j.jasrep.2015.08.041

National Centers for Environmental Information (NCEI). Pacific Decadal Oscillation (PDO). Retrieved November 29, 2021, from https://www.ncdc.noaa.gov/teleconnections/pdo/.

Phillips RC (1984). The ecology of eelgrass meadows in the Pacific Northwest: A community profile. US Fish Wildlife Service FWS/OBS-84/24.

Ruckelshaus, MH (1994). Ecological and genetic factors affecting population structure in the marine angiosperm, Zostera marina L [Doctoral dissertation, University of Washington]

Short F, Coles R, McKenzie LJ, & Finkbeiner MA (2008). Methods for mapping Seagrass Distribution. In *Global Seagrass Research Methods* (pp. 101–119). essay, Elsevier.

Sullivan BK, Trevathan-Tackett SM, Neuhauser S, & Govers LL (2018). Review: Host-pathogen dynamics of seagrass diseases under future global change. *Marine Pollution Bulletin*, *134*, 75–88. https://doi.org/10.1016/j.marpolbul.2017.09.030

Temperature products. National Centers for Environmental Information (NCEI). (2021, October 22). Retrieved November 24, 2021, fromhttps://www.ncei.noaa.gov/monitoring/temperature.

Traganos D, Poursanidis D, Aggarwal B, Chrysoulakis N, Reinartz P (2018). Estimating Satellite-Derived Bathymetry (SDB) with the Google Earth Engine and Sentinel-2. *Remote Sensing*, 10(6):859. https://doi.org/10.3390/rs10060859

Unsworth RKF, Collier CJ, Waycott M, Mckenzie LJ, & Cullen-Unsworth LC (2015). A framework for the resilience of Seagrass Ecosystems. *Marine Pollution Bulletin*, *100*(1), 34–46. https://doi.org/10.1016/j.marpolbul.2015.08.016

Walker WH, Meléndez-Fernández OH, Nelson RJ, & Reiter RJ (2019). Global climate change and invariable photoperiods: A mismatch that jeopardizes animal fitness. *Ecology and Evolution*, *9*(17), 10044–10054. https://doi.org/10.1002/ece3.5537

Washington Department of Natural Resources – WADNR (2020). Nearshore Habitat eelgrass monitoring*: WA - DNR*. WA. (n.d.). Retrieved November 10, 2021, from https://www.dnr.wa.gov/programs-and-services/aquatics/aquatic-science/nearshore-habitat-eelgrass-monitoring.

Waycott M, Duarte CM, Carruthers TJ, Orth RJ, Dennison WC, Olyarnik S, Calladine A, Fourqurean JW, Heck KL, Hughes AR, Kendrick GA, Kenworthy WJ, Short FT, & Williams SL (2009). Accelerating loss of seagrasses across the globe threatens coastal ecosystems. *Proceedings of the National Academy of Sciences*, *106*(30), 12377–12381. https://doi.org/10.1073/pnas.0905620106